# Surface and Near-surface Moisture Content Assessment using Multi-Temporal Satellite Images over Perak Tengah and Manjung Regions, Malaysia

**Abdalhaleem A. Hassaballa[1*], Abdul Nasir B. Matori[1], Helmi Z. M. Shafri[2]**

1. Geoinformatics and Highway Cluster, Department of Civil Engineering, Universiti Tecknologi PETRONAS, Bandar Seri Iskandar, 31750, Tronoh, Perak Darul Ridzuan, Malaysia.
2. Department of Civil Engineering, Faculty of Engineering, University Putra Malaysia, 43400, Serdang, Selangor Darul Ehsan, Malaysia.
   *corresponding author's e-mail: halimhasbo@hotmail.com

**Abstract**. Soil moisture is considered as the most significant boundary condition controlling precipitation, especially in the semi-arid zones. On the regional scale, the importance of soil moisture appears in agricultural assessment (crops yield management, irrigation management, etc.), flood and draught control. Based on these principles, the study was carried out to estimate surface moisture content ($\theta$) over Perk Tengah and Manjung districts in Malaysia using optical images from multi-temporal satellites which are NOAA/AVHRR and MODIS. In order to generate the moisture maps, "Universal Triangle" algorithm was used for NOAA/AVHRR based on land Surface Temperature (Ts) and the Normalized Difference Vegetation Index (NDVI) extracted from images beside field measurements of $\theta$. $\theta$ also estimated from MODIS through the extraction of soil wetness index (SWI) which is a sensitive parameter that controls the mechanism of land surface and the processes at the atmosphere. Throughout the study area, $\theta$ was measured using soil moisture probe for some parts of the study area and the oven method for the others; both Ts and $\theta$ were measured at time of satellites overpass in two different near surface depths 5 cm and 10 cm to examine the depth influence on $\theta$ and Ts magnitudes. The study area was divided into three basic classes according to the nature of surface cover which were: urban area, agricultural area and multi-types surface cover area. Moisture content maps were generated from both satellites for each surface cover type then; generalized moisture maps were produced through correlating the three different surface cover types for each satellite using weightage method. Finally, two sets of validation were applied to the resultant moisture maps. Firstly, experimental validation was performed between the satellites estimated $\theta$ and $\theta$ values measured in-situ. Good relationships were found with $R^2$ reached 0.79 and 0.76 for NOAA and MODIS sensors respectively. Secondly, a success rate curve based on spatio-statistical technique was used for validating the generalized maps in order to study the high-low distribution of $\theta$ within NOAA and MODIS generalized maps. The resultant validation reflected a high compatibility represented by area under curve of (0.81) 80%.

## 1. Introduction

Surface moisture content acts as an extremely substantial part in land surface hydrology, so it regulates the excess rainfall into run off and infiltration. Coupled with surface temperature, it influences the depth of planetary boundary layer, wind patterns [1] and regional water energy budgets. The principal factor in the determination of wet or dry anomalies over huge continental regions throughout the

summer time is because of the recycling of the water as a result of moisture content, evapotranspiration and rainfall [2, 3]. Soil moisture content can be considered as the most crucial boundary condition maintaining summer precipitation within the semi-arid zones[4]. For a regional scale, the significance of soil moisture seems to be in agricultural evaluation (crops yield management, irrigation management, etc.), flood and draught management[5, 6].

## 1.1. *Application of Soil Moisture*
Among the parameters of the hydrologic cycle, the most significant element is the soil moisture since it has an influence on climatic change over land and also plays the identical role over land as sea surface temperature plays over oceans and seas. In certain situations, it offers great possibilities of storing the atmospheric energy transferred to it via rainfall (monthly), consequently, transferring them back to the atmosphere via evaporation and influencing the climate [7]. Soil moisture helps in the redistribution of precipitation into surface runoff and subsurface run off [8]. Furthermore, soil moisture content has an effect on the soil erosion, soil aeration, distribution and growth of vegetation, soil microbial activity, the concentration of toxic substances, the motion of nutrients inside the soil towards the roots and weather forecast at a local to regional scale[9]. Far away from these, there are lots of other real world applications that soil moisture regulates, that make it an essential factor to determine. The examples below have been pointed out because of their impacts on human life:

*Monitoring of drought and flood-* quantity of soil moisture can easily affect the hydrologic drought and flooding since they're strongly linked to its availability in particular region. The shortage in root zone soil moisture for many periods of time, results in hydrologic drought later will result in agricultural drought. Alternatively, when rainfall excesses a bit longer time, soil gets saturated with water resulting in flooding, particularly for instant heavy rainfall that doesn't give sufficient time for perceptible water to percolate beneath soil and therefore produces high run-off and flash flooding [10].

*Hydrologic modeling* - the evaluation of soil water change as a result of natural and anthropogenic causes is very essential. Because soil moisture is often a primary element of water cycle, it can be beneficial to analyze water cycle processes, precipitation and discharge routine analysis via getting the volume of soil water content.

*Civil Engineering* - the large structural properties are extremely affected by soil water since it makes soil heavier and much softer to carry them. Therefore, it's very necessary and essential to understand and handle the moisture quantity and deviation of the soil water through years. This could help in sustaining the engineering structures such as dams, bridges, roads, etc. which are properly ideal for the soil conditions. Among the wide range of soil moisture applications in urban, the flood forecast is dependent on the spatial distribution of the saturation of ground soil [11, 12].

*Agriculture and Modeling of crop system-* Agriculture is considered the most reliant on soil moisture and irrigation, especially in the dry seasons in the event the rainfall is scarce. It is vital and necessary to understand the level of moisture within the root zone prior to cultivating any crop. That can assist farmers to choose whether they need to plant a specific crop or not [13].

## 1.2. *Problem statement*
Due to the spatial and temporal variation of soil moisture it can be considered as a crucial hydrological factor containing direct impacts on agriculture, forest ecology, civil engineering, water resources management, and crop system modeling as mentioned in the earlier sections. When improperly described, it results in the mistaken evaluation of the other hydrology as well as cycle parameters. Researchers have been attempting to identify the physical connection among the soil moisture and various ecosystem elements (e. g. precipitation, runoff, elevation, soil type, vegetation etc.).

This paper is aiming at (1) representing the usefulness of the Optical/Thermal Infrared remote sensing data and land-use information in soil moisture content (θ) estimation using MODIS and NOAA satellites which enjoy high temporal resolution for daily moisture monitoring beside, (2) generating a generalized soil moisture map by correlating three different moisture maps obtained from three dissimilar covers along the study area to simulate the reality of surface cover within the study area.

## 2. The Study Area

Perak Tengah & Manjung are part of Perak state lay between latitude $4^o00`$ – $4^o30`$ N and longitude $100^o30`$ – $101^o00`$ E (figure 1), with an area of 2,400 square kilometers. MODIS (Terra & Aqua) images (from June – September 2012) were acquired for θ algorithms generation. Three stations were selected throughout the study area in terms of their variety in environmental and vegetation cover explained as Sitiawan to represent urban area with impervious surfaces, Utp represent a mixed surface cover type and Seberang Perak represents agricultural land.
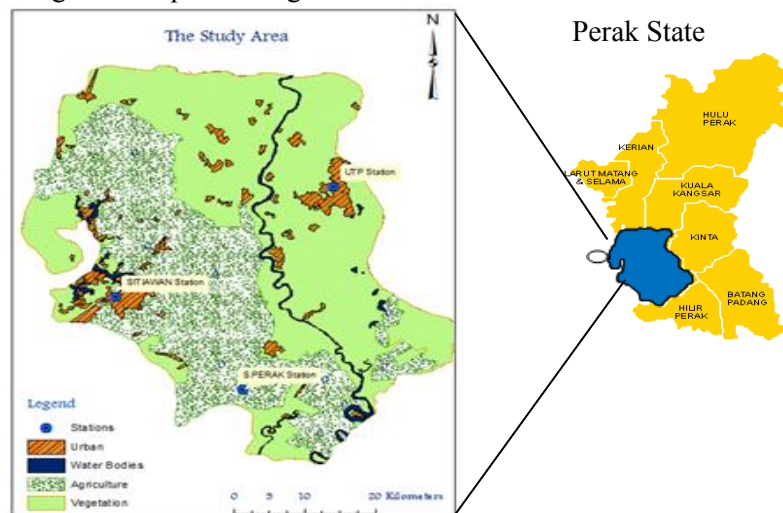


Figure 1: The study area with classified map for surface cover types representation.

## 3. Materials and Methods

### 3.1. *Data Collection and Processing*

NOAA/AVHRR 17&18 images (from February – April 2011) were acquired for θ algorithms generation. Three locations were selected throughout the study area in terms of their variety in the environment and vegetation cover represented by Sitiawan to stand for urban area, Seberang Perak paddy field represents the agricultural lands, UTP station represents a mixed surface cover type. MODIS Land Surface Temperature and Emissivity (LST/E) which are products of Aqua MODIS (e.g. MYD11A1 products) and Terra-MODIS (e.g. MOD11A1 products) offered per-pixel temperature and emissivity values every day. MODIS scientific information is availed to the public through various World Wide Web sites and FTP records.

In order to process the acquired satellite's images for surface temperature and emissivity extraction, subset area has been delineated surrounding each weather station and any spatial computation performed within each subset area was assumed to represent the average value of the sub area pixels. On the other hand, in-situ measurements of Ts and θ were conducted during the satellite's overpassing time using mini thermometer and a NETRON 740 soil moisture probe respectively.

### 3.2. *Split-window algorithm for deriving NOAA Ts*

The general form of the split-window equation can be written as [14]:

$$T_S = T_4 + A(T_4 - T_5) + B \tag{1}$$

Ts represents the land surface temperature, T4 and T5 represent the brightness temperature for channel 4 and 5 respectively, A and B are the coefficients determined by the impact of atmospheric conditions and other related factors on the thermal spectral radiance transmission in channels 4 and 5.

### 3.3. *Normalized Difference Vegetation Index  NDVI*

The NDVI measurements were made with a combined red and near-infrared radiometer, developed at NASA/Goddard Space Flight Centre, which measures the reflected radiation in the bands (0.58-0.68 µm) and (0.73-1.1 µm):

$$NDVI = \frac{(NIR - RED)}{(NIR + RED)} \tag{2}$$

MODIS's Surface temperature values over study area for the entire period were downloaded directly from web source (http://ladsweb.nascom.nasa.gov/), which is a web interface to the Level 1 and Atmosphere Archive and Distribution System (LAADS).

### 3.4. *Soil Moisture Estimation*

*3.4.1. Universal Triangle. The* A simple regression relationship between θ, Ts and NDVI to predict the moisture profile from near-surface  through different soil depths is achieved according to the Universal Triangle theorem which explains that "there is a unique relationship among soil moisture, vegetation cover, and surface temperature for a given region [15, 16]. [15] found that the relationship between soil moisture θ, NDVI*, and Ts* can be expressed through a regression formula such as:

$$\theta = \sum_{i=0}^{i=n} \sum_{j=o}^{j=n} a_{ij} NDVI^{*(i)} T^{*(j)} \tag{3}$$

In terms of a second order polynomial, the above equation can be expanded as:

$$\theta = a_{00} + a_{10}NDVI^* + a_{20}NDVI^{*2} + a_{01}T^* + a_{02}T^{*2} + a_{11}NDVI^*T^* + a_{22}NDVI^{*2}T^{*2} + a_{12}NDVI^*T^{*2} + a_{21}NDVI^{*2}T^* \tag{4}$$

$$T^* = \frac{T - T_o}{T_S - T_o} \tag{5}$$

$$NDVI^* = \frac{NDVI - NDVI_o}{NDVI_S - NDVI_o} \tag{6}$$

Ts and NDVI are observed land surface temperature and normalize difference vegetation index, respectively, and the subscripts o and s stand for minimum and maximum values.

*3.4.2. Thermal Inertia (TI) for MODIS moisture content.* Many models have been produced using the thermal inertia technique by [17, 18] and [19] for soil moisture extraction depending on the concept that, water bodies possess a higher thermal inertia (TI) than dry soils. Within produced methods, apparent thermal inertia (ATI, presumed homogeneous layer for TI) is utilized. ATI is inferred through the measurements of spectral surface albedo and also the diurnal temperature range. It signifies the temporal and spatial variation of soil and canopy moisture [20]. The greater ATI, the greater the moisture content of the surface. The basic to derive soil water content is based on the idea that high/low ATI values match maximum/minimum soil moisture contents [21]. By including the soil wetness index (SWI). The soil wetness index (SWI) for a given day or time (t), which represents relative surface soil moisture, is described as:

$$SWI_{(t)} = \frac{Ts_{max(i)} - Ts_{(i)}}{Ts_{max(i)} - Ts_{min}} \tag{7}$$

Where $Ts_{(i)}$ is the land surface temperature of i-th pixel. $Ts_{(min)}$ is the minimum LST while in the triangle which specifies the wet edge. $Ts_{(max)}$ would be the maximum LST for i-th NDVI.

To maintain simplicity and consistency in method across various scales, the dry edge was modeled using a linear empirical fit to NDVI:

$$Ts_{max(i)} = a + bNDVI_{(i)} \tag{8}$$

By having the upper ($\theta_{max}$) and lower ($\theta_{min}$) boundaries of volumetric soil moisture within the surface, the wetness index ($SWI_{(t)}$) over a given day or time could be transformed into a complete estimate of volumetric surface soil moisture ($\theta_v$) making use of the following relationship [22]

$$\theta_v = \theta_{min} + SWI_{(t)}(\theta_{max} - \theta_{min}) \tag{9}$$

$\theta_{max}$ is the upper limit of $\theta_v$ and will undertake values between field capacity (FC) and $\theta_{min}$ is the lower limit of $\theta_v$ and could be symbolized as permanent wilting point (PWP).

In order to determine the upper and lower moisture values which represented in the soil's field (FC) capacity and the permanent wilting point (PWP) respectively, samples were collected from the soil of each type of the surface cover among the three selected partitions of the study area (full vegetated, urban and multi-cover surfaces). A particle size distribution (PSD) test was applied to the collected samples using (Master-sizer 2000 device) provided by UTP meteorological station. Consequently, soil's structure was classified into the standard classes (sand, silt and clay) with different percentages for surface cover type. Afterward, a hydraulic properties calculator, which is open-source software based on the physical concept of soil water characteristics triangle produced by the U.S. Department of Agriculture (USDA), was used to determine (FC) and (PWP) according to sand and clay percentage.

3.5. *Derivation of generalized moisture map*

The concept of the generalized map derivation is based fundamentally on the estimation of a pixel-based moisture content value, within which, variable surface cover types share the spectral signatures to generate the moisture. Based on that, weightage of each of the three different cover types was determined and imposed in the generalized map formation. Firstly, satellite's surface moisture maps were generated using a pixel-based SWI in addition to the FC and PWP from each of the three stations, in which, the moisture map at pixel (i) level using the moisture boundaries over Utp station took the value of $\theta_{UTP_i}$, same tasks went with the moisture images generated over Sitiawan and Seberang perak which represented by $\theta_{SITI_i}$ and $\theta_{SP_i}$ respectively. The total moisture map of the pixel based image was calculated as a summation of the three moisture values for each pixel ($\theta_{SUM_i}$) then, the fraction ($Fr_i$) of station's moisture share within the pixel was calculated as a percentage of the pixel moisture value of the particular station to the total moisture at the pixel. Equations (10) to (13) below describe mathematically the steps towards the generalized moisture estimation over the study area.

$$\theta_{SUM_i} = \sum_{i=1}^{n} (\theta_{UTP_i}, \theta_{SITI_i}, \theta_{SP_i}) \tag{10}$$

$$Fr_{UTP_i} = \frac{\theta_{SITI_i}}{\theta_{SUM_i}} ; Fr_{SITI_i} = \frac{\theta_{UTP_i}}{\theta_{SUM_i}} ; Fr_{SP_i} = \frac{\theta_{SP_i}}{\theta_{SUM_i}} \tag{11}$$

The weightage ($W_i$) of each surface cover type for the single pixel was determined by applying the fraction of each station to the corresponding full moisture pixel which was generated by own boundaries (FC & PWP). Finally, the generalized moisture ($\theta_i$) for each image pixel was calculated as a summation of the three different weightages of pixel's moisture.

$$W_{UTP_i} = Fr_{UTP_i} \times \theta_{UTP_i} ; W_{SITI_i} = Fr_{SITI_i} \times \theta_{SITI_i} ; W_{SP_i} = Fr_{SP_i} \times \theta_{SP_i} \tag{12}$$

$$\theta_i = W_{UTP_i} + W_{SITI_i} + W_{SP_i} \tag{13}$$

## 4. Results and Discussion

The Generalized moisture content maps were extracted as a correlation between the 3 different covers which are: the urban areas represented by Sitiawan station, the agricultural area represented by Seberang Perak paddy field and the multiple surface cover represented by Utp station. NOAA 17 moisture content map was generated benefiting from parameters of daily moisture content measured in-situ at 5 cm depth in conjunction with images acquisition time; this map is a sort of raster image produced by ArcGIS software in which each pixel represents a value of moisture content. On the other hand, MODIS moisture map was retrieved from thermal inertia method at the same NOAA acquisition time to enable the study of their spatial accuracy using success rate validation. Figure 2 below show the resultant generalized moisture maps produced by the two sensors using to different methods.
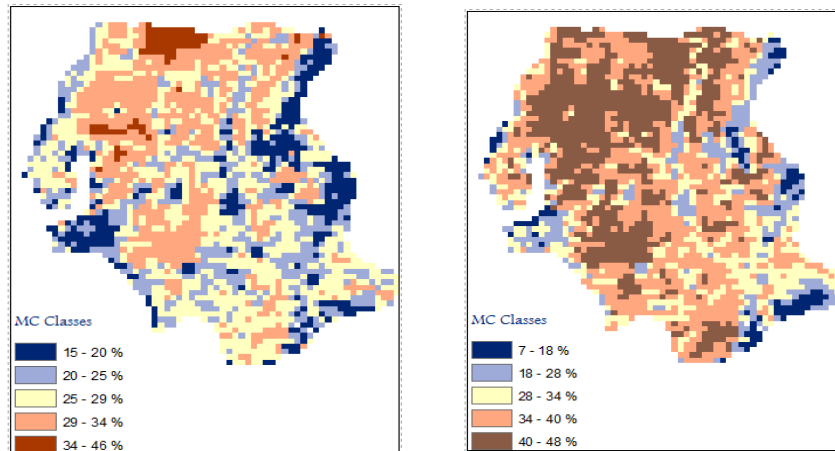
Figure 2: Generalized moisture maps of the 3 locations from NOAA 17(left) and MODIS T. (right).

### 4.1. *Moisture content validation*

In the course of this study, two types of validations were used on moisture content assessed values. The first type was an experimental validation, whereas the satellite's moisture content values which were extracted from the reserved images, were plotted against the reserved in-situ moisture values in terms of point measurements. The second type was a spatial validation for the pixel-based estimations of moisture content, which was accomplished using the Success Rate technique.

Figure 3 below represents the validation of generalized moisture maps used in the form of point measurements, where the field moisture values were correlated against the satellites moisture generated from Ts and NDVI. The success rate was used as a spatial validation method in the study, which was applied to the generalized moisture maps by comparing the highest/lowest moisture content zone with the adjacent moisture content with different image (image from different satellite).
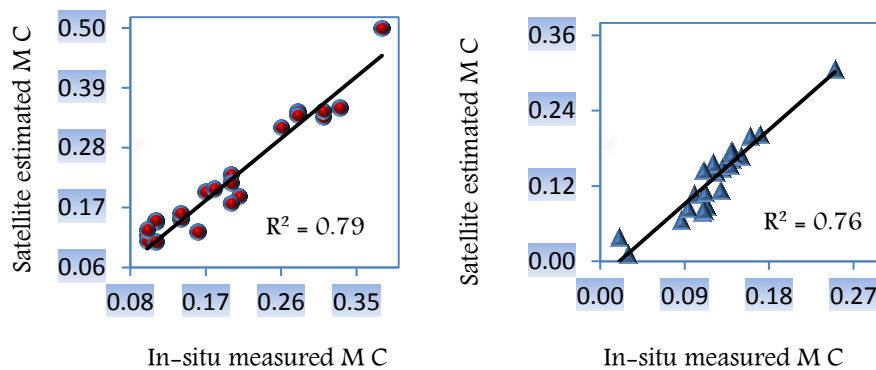


Figure 3: Validation of generalized moisture content using NOAA17 (left) and MODIS T. (right).

The success rate curves were created and their areas under the curve AUC were calculated. The rate explains how well the highest/lowest moisture values meet each other [22]. So, the area under curve can assess the prediction accuracy qualitatively. To obtain the relative ranks for each prediction pattern, the calculated index values of all cells in the study area were sorted in descending order using Quantile Classification task in ArcGIS environment. Figure 4 below shows the resultant AUC, in which MODIS moisture map was used as base (Moisture Occurrence index %) and NOAA moisture high class was used as points (Cumulative M.C Occurrences %).

It is obvious from all of the generated moisture maps that, the vegetated areas within the study area are most likely to carry much moisture content than the built up areas as well as the bare soils. This could be seen most obviously in the agricultural fields so that, the area at those fields is covered by vegetation which is uniformly growing. The high moisture value is noticed over the uniform green areas in all scenes. This justified as:
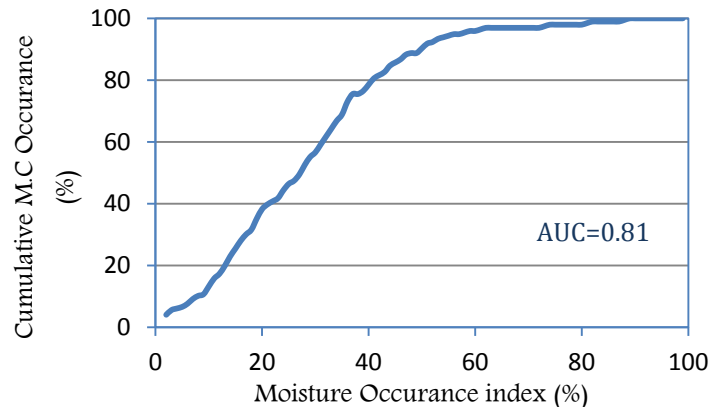
Figure 4: The area under curve of high moisture content class of NOAA VS MODIS as a base map.

Moisture content over the built up areas is easily lost by evaporation because the surface is exposed to the direct sun illumination, wind and most of the weathering parameters, while soils under the vegetated areas are shadowed by the leaves against the sun impact and weathering effects.

From the spatial patterns and distribution of the soil moisture content of the two satellites (NOAA & MODIS) it can be observed that, in almost all images moisture showed close resemblance with slide differences in moisture values and distribution, this change is justifiable because, the overpassing time for NOAA 17 (10:00 -10:30 AM) is a bit earlier than MODIS Terra (10:45 -11:30 AM) at the study area's local time so, this considered as quite enough time for surface moisture to get fluctuated.

Spatial validations were performed in order to assure the adjacency of the acquired optical/infrared images to each other in retrieving the value and distribution of the surface moisture content with regard to the land uses/cover variability.

## 5. Conclusion

The generalized moisture map was calculated upon a pixel-base weighting. So that, the participation of each land surface cover within the image pixel could be imposed in a try to surpass the limitation of the coarse resolution that justifies the limited usage of MODIS images as well as the satellites those have typical resolutions. In addition, the technique managed to express the status of moisture content at the surface taking into account the variable soil textures and their holding capacities through encompassing FC and PWP of the soil profiles into a single pixel.

Validation produced a reasonable connection with a high significance between moisture estimated over the agricultural land of Seberang Perak and its in-situ measurements is exist, this could be attributed to the uniformity of the vegetation cover represented in the cultivated crops the which tend to reduce the Ts values producing a relatively high SWI over the entire area. On the other hand, a moderate relationship was found between the two sets of moisture content over Sitiawan area (built up area), this is certainly because soils over the urban areas get impervious due to compaction beside other activities. Away from that, the third part which is occupied by partial vegetation cover shared with scattered patches of agricultural fields beside some residential areas produced a significant correlation along the distributed surface covers.

## References
[1]     Zhang, J. and Crowley, T. J., 1989. Historical climate records in China and reconstruction of past climates. *J. Clim.* vol. 2, pp.
[2]     Bindlish, R., 2000. Active and passive microwave remote sensing of soil moisture. Ph.D, Civil and Environmental Engineering, The Pennsylvania State University, Graduate School.
[3]     Hassaballa,  A. A. and Matori, A. B., 2011. Study on surface moisture content, vegetation cover and air temperature based on NOAA/AVHRR surface temperatures and field measurements. *IEEE.* pp. 1-5.

[4] Beljaars, A. C. M. Viterbo, P., Miller, M. J., Betts, A. K., 1996. The anomalous rainfall over the United States during July 1993: Sensitivity to land surface parameterization and soil moisture anomalies. *Mon. Weather Rev.*, vol. 124, pp. 362-383.

[5] Hassaballa, A. A. Althuwaynee, O. F., Pradhan, B., 2013. Extraction of soil moisture from RADARSAT-1 and its role in the formation of the 6 December 2008 landslide at Bukit Antarabangsa, Kuala Lumpur. *Arabian J. Geosci.* 1-10.

[6] Hassaballa, A. A., Matori, A. B., 2011. The estimation of air temperature from NOAA/AVHRR images and the study of NDVI-Ts impact: Case study: The application of split-window algorithms over (Perak Tengah & Manjong) area, Malaysia. *IEEE*, pp. 20-24.

[7] Martínez-Fernández, J., Ceballos, A., 2003. Temporal stability of soil moisture in a large-field experiment in Spain. *Soil Sci. Soc. Am. J.* 67, 1647-1656.

[8] Pauwels, V., Hoeben, R., Verhoest, N. E. C., De Troch, F. P., Troch, P. A., 2002. Improvement of TOPLATS based discharge predictions through assimilation of ERS based remotely sensed soil moisture values. *Hydrol. Processes.* 16, 995-1013.

[9] Koster, R. D., Suarez, M. J., Liu, P., Jambor, U., Berg, A., Kistler, M., Reichle, R., Rodell, M., Famiglietti, J., 2004. Realistic initialization of land surface states: Impacts on subseasonal forecast skill. *J. Hydrometeorol.* 5, 1049-1063.

[10] Sahoo, A. K., 2008. Improvement of soil moisture prediction through AMSR-E data assimilation. Graduate Faculty. *PhD. George Mason University*, USA,

[11] Entekhabi, D., Nakamura, H., Njoku, E. G., 1994. Solving the inverse problem for soil moisture and temperature profiles by sequential assimilation of multifrequency remotely sensed observations. *IEEE Trans. Geosci. Remote Sens.* 32, 438-448.

[12] Su, Z., Troch, P. A., de Troch, F. P., Nochtergale, L., Cosyn, B., 1995. Preliminary Results of Soil Moisture Retrieval From ESAR (EMAC 94) and ERS-1/SAR, Part II: Soil Moisture Retrieval., pp. 7-19.

[13] Western, A. W., Green, T. R., Grayson, R. B., 1997. Hydrological modelling of the Tarrawarra Catchment: Use of soil moisture patterns. pp. 8-11.

[14] Becker, F., Li, Z.-L., 1990. Temperature-independent spectral indices in thermal infrared bands. *Remote Sens. Environ.* 32, 17-33.

[15] Carlson, T. N., Gillies, R. R., Perry, E. M., 1994. A method to make use of thermal infrared temperature and NDVI measurements to infer surface soil water content and fractional vegetation cover. *Remote Sensing Reviews*. 9, 161-173.

[16] Gillies, R. R., Kustas, W. P., Humes, K. S., 1997. A verification of the 'triangle' method for surface soil water content and energy fluxes from remote measurements of the Normalized Difference Vegetation Index NDVI and surface. *Int. J. Remote Sens* 18, 3145-3166.

[17] Xue, Y., Cracknell, A. P., 1995. Advanced thermal inertia modelling. *Remote Sensing*. 16, 431-446.

[18] Sobrino, J. A., El Kharraz, M. H., 1999. Combining afternoon and morning NOAA satellites for thermal inertia estimation 2. Methodology and application. *J. Geophys. Res.* 104, 9455-9465.

[19] Mitra, D. S., Majumdar, T. J., 2004. Thermal inertia mapping over the Brahmaputra basin, India using NOAA-AVHRR data and its possible geological applications. *Int. J. Remote Sens.* 25, 3245-3260.

[20] Tramutoli, V., Claps, P., Marella, M., Pergola, N., Sileo, C., 2000. Feasibility of hydrological application of thermal inertia from remote sensing. pp. 16-18.

[21] Western, A. W., Green, T. R., Grayson, R. B., 1997. Hydrological modelling of the Tarrawarra Catchment: Use of soil moisture patterns., pp. 8-11.

[22] Wagner, W., Lemoine, G., Rott, H., 1999. A method for estimating soil moisture from ERS scatterometer and soil data. *Remote Sens. Environ.* 70, 191-207.